



Published in final edited form as:

*Nat Neurosci.* 2008 January ; 11(1): 62–71.

## A thermosensory pathway that controls body temperature

**Kazuhiro Nakamura and Shaun F. Morrison**

*Neurological Sciences Institute, Oregon Health & Science University, 505 N.W. 185th Avenue, Beaverton, OR 97006, USA*

### Abstract

Defending body temperature against environmental thermal challenges is one of the most fundamental homeostatic functions governed by the nervous system. Here we show a novel somatosensory pathway, which essentially constitutes the afferent arm of the thermoregulatory reflex triggered by cutaneous sensation of environmental temperature changes. Using rat *in vivo* electrophysiological and anatomical approaches, we revealed that lateral parabrachial neurons play a pivotal role in this pathway by glutamatergically transmitting cutaneous thermosensory signals received from spinal somatosensory neurons directly to the thermoregulatory command center, preoptic area. This feedforward pathway mediates not only sympathetic and shivering thermogenic responses but also metabolic and cardiac responses to skin cooling challenges. Notably, this ‘thermoregulatory afferent’ pathway exists in parallel with the spinothalamocortical somatosensory pathway mediating temperature perception. These findings make an important contribution to our understanding of both the somatosensory system and thermal homeostasis—two mechanisms fundamental to the nervous system and to our survival.

---

Even during rapid changes in environmental temperature, the body temperature of homeothermic animals, including humans, is maintained within the narrow range necessary for optimal cellular and molecular functions. How the nervous system functions to defend body temperature against environmental thermal challenges remains a fundamental question in physiology<sup>1,2</sup>. The preoptic area (POA) is the thermoregulatory center providing command signals descending to peripheral effectors<sup>1,3–6</sup>. To evoke behavioral, autonomic, somatic and hormonal responses counteracting changes in environmental temperature before they impact body core temperature, thermoregulatory command neurons in the POA need to receive feedforward signaling of environmental temperature information from skin thermoreceptors through the spinal and trigeminal dorsal horns<sup>3,5–8</sup>. However, the neural substrate for the ascending thermoregulatory feedforward pathway, especially the essential central mechanism linking the second order somatosensory neurons in the dorsal horn to the POA has yet to be identified.

The best-known central pathway for somatosensory signaling of cutaneous thermal sensation is the spinothalamocortical pathway, in which signals from skin thermoreceptors are transmitted through a direct projection from the dorsal horn to the thalamus and then relayed to the primary somatosensory cortex<sup>9,10</sup>. Although the spinothalamocortical pathway is responsible for perception and discrimination of cutaneous temperature<sup>9,10</sup>, it is unknown whether this pathway contributes to homeostatic responses against changes in environmental

---

Correspondence should be addressed to K.N. (nakamura@ohsu.edu).

#### AUTHOR CONTRIBUTIONS

K.N. contributed to most of the experimental design, performed the experiments and analyzed the data. K.N. and S.F.M. discussed the data and wrote the paper.

#### COMPETING INTERESTS STATEMENT

The authors declare no competing financial interests.

temperature, for instance, by providing thermosensory signals to the POA through collaterals from the thalamic relay neurons.

The major aim of the present study is to identify the somatosensory pathways responsible for the defense of homeostasis against environmental thermal challenges. Using *in vivo* electrophysiological and anatomical approaches, we first sought to identify neuronal populations that provide cutaneous thermal signals directly to the POA and then to investigate the functional role of these candidate neuronal populations in thermoregulatory, metabolic and cardiovascular responses to changes in skin temperature. Furthermore, we examined the involvement of the spinothalamocortical somatosensory pathway in thermoregulatory autonomic responses.

## RESULTS

### Neurons providing thermosensory signals to the POA

Candidate populations of neurons providing thermosensory signals directly to the POA were identified as those both retrogradely labeled from the POA and expressing Fos protein, a marker of activated neurons<sup>11</sup>, following exposure to a cold environment. The retrograde tracer, cholera toxin b-subunit (CTb) was injected into a subregion of the rat POA covering the median preoptic nucleus (MnPO) and periventricular POA (Fig. 1a,b and Supplementary Fig. 1a,b). Subsequent exposure of the animals to a 4°C environment for 4 h induced a prominent expression of Fos in many CTb-labeled neurons in the lateral parabrachial nucleus (LPB) that was markedly enhanced in comparison to that in animals exposed to 24°C (Fig. 1c–f). CTb-labeled neurons were distributed in the external lateral (LPBel), central (LPBc) and dorsal (LPBd) subnuclei of the LPB and cooling-evoked Fos induction in these CTb-labeled neurons was significant in the LPBel and LPBc, but not in the LPBd (Supplementary Fig. 1c–e). No other brain regions, including the thalamus, contained a substantial number of CTb-labeled neurons that also expressed Fos after cold exposure.

Since LPB neurons project broadly to the whole POA, the bed nucleus of the stria terminalis (BST), paraventricular hypothalamic nucleus (PVH) and dorsomedial hypothalamus (DMH)<sup>12–15</sup>, we further examined the extent to which thermosensory inputs from the LPB terminate in POA subregions lateral to the MnPO or in other hypothalamic regions. Although many retrogradely labeled cells were found in the LPB following CTb injections in the medial or lateral POA, BST, PVH or DMH, the percentages of Fos-positive cells in the CTb-labeled populations in the LPBel and LPBc after cold exposure (4–38%, counted in the LPBel) were markedly lower than those when CTb injections were centered in the MnPO and periventricular POA (62–81%; Supplementary Fig. 2) and neither the LPBd nor any other brain regions had substantial numbers of CTb-labeled neurons that expressed Fos after cold exposure. These results indicate that neurons in the LPBel and LPBc are the sole source of skin cooling-activated inputs to the POA and that these LPB subregions provide thermosensory inputs more densely to the median subregion of the POA than to the medial and lateral POA subregions, BST, PVH or DMH. Furthermore, these anatomical observations prompted us to the following physiological and anatomical investigations to test the hypothesis that cooling-activated POA-projecting LPB neurons represent the link between dorsal horn neurons and the POA in the thermosensory pathway to defend body temperature during the challenge of reduced environmental temperature.

### Dorsal horn neurons innervate POA-projecting LPB neurons

Environmental temperature is sensed by the action of transient receptor potential channels in the cutaneous terminals of primary somatosensory neurons that convey these thermal signals to second order somatosensory neurons in the dorsal horn<sup>16</sup>, which provide numerous

projections to the LPB<sup>17–19</sup>. Thus, we injected the retrograde tracer, Fluoro-Gold, into the POA and the anterograde tracer, *Phaseolus vulgaris* leucoagglutinin (PHA-L), into the spinal dorsal horn (Fig. 1g,h) and found that many PHA-L-labeled axon fibers derived from dorsal horn neurons were distributed among Fluoro-Gold-labeled POA-projecting neurons clustering in the LPBel and LPBc (Supplementary Fig. 3a). Confocal laser-scanning microscopy revealed close appositions of the axon swellings of dorsal horn neurons to PSD-95-positive postsynaptic structures of POA-projecting LPB neurons (Fig. 1i and Supplementary Fig. 3b). No such appositions were found in the thalamus or the nucleus of the solitary tract, structures which receive numerous projections from the dorsal horn.

### Unit recording of LPB neurons projecting to the POA

Using an *in vivo* unit recording technique, the responses to thermosensory input from the skin were examined in single POA-projecting LPB neurons (Fig. 2). We used collision tests to determine whether LPB neurons were antidromically activated by electrical stimulation in the MnPO (Fig. 2b,c,g). Of 14 antidromically identified LPB neurons projecting to the POA, 11 neurons increased their firing rates in response to trunk skin cooling (resting,  $2.2 \pm 0.9$  spikes  $\cdot 10$  s<sup>-1</sup>; peak value during cooling,  $27.8 \pm 6.0$  spikes  $\cdot 10$  s<sup>-1</sup>; expressed as mean  $\pm$  s.e.m. throughout paper,  $P < 0.005$ , two-tailed paired *t*-test; cool-responsive neuron). These dramatic increases in firing rate were seen as the skin was cooled in the range between  $36.6 \pm 0.3^\circ\text{C}$  and  $34.4 \pm 0.3^\circ\text{C}$ . The skin cooling-evoked increases in LPB neuronal discharge were rapidly reversed following the onset of skin rewarming. The changes in LPB neuronal firing rate paralleled skin cooling-evoked increases in sympathetic nerve activity (SNA) to the thermogenic organ, brown adipose tissue (BAT) (Fig. 2a). The average antidromic latency and estimated conduction velocity of these cool-responsive neurons were  $20.9 \pm 0.9$  ms and  $0.45 \pm 0.02$  m  $\cdot$  s<sup>-1</sup>, respectively. The remaining 3 antidromically activated neurons showed no clear thermoresponsive changes in their firing rate (pre-cooling:  $23.8 \pm 10.8$  spikes  $\cdot 10$  s<sup>-1</sup>; highest value during cooling:  $28.8 \pm 6.8$  spikes  $\cdot 10$  s<sup>-1</sup>;  $P > 0.05$ ; non-thermoresponsive neuron).

To test whether firing rate of these cool-responsive LPB neurons was correlated with skin temperature during cooling, linear regression analysis was performed for each cool-responsive neuron (Supplementary Fig. 4). The firing rate of each cool-responsive LPB neuron showed a significant, negative correlation with skin temperature and the average responsiveness (slope) of the relationship between the discharge frequency of cool-responsive neurons and skin temperature was  $-8.9 \pm 1.9$  spikes  $\cdot 10$  s<sup>-1</sup> per  $^\circ\text{C}$ . In contrast, none of the non-thermoresponsive LPB neurons showed a significant correlation between firing rate and skin temperature.

Since the LPB may also mediate pain-related signals<sup>20</sup>, we tested the responsiveness of the LPB neurons to a noxious tail pinch stimulation. No response to noxious tail pinch was observed in 7 of 8 cool-responsive LPB neurons and 1 of 2 non-thermoresponsive neurons, although a rapid pressor response was observed in all trials (Fig. 2e). The two neurons that responded to tail pinch showed a high frequency burst discharge in response to pinching (Fig. 2f). Each recorded LPB neuron was localized with juxtacellularly labeling: cool-responsive neurons were located in the LPBel (Fig. 2d,h). These results indicate that neurons distributed in the LPBel are activated by cool signals from the skin, but not by noxious mechanical stimuli, and that they transmit these thermal signals to the POA.

### Critical role of LPB–POA pathway in thermal homeostasis

To test the hypothesis that the LPB neurons activated by cool signals from the skin mediate physiological thermoregulatory responses, we examined *in vivo* the effect of inhibition of neurons or blockade of glutamatergic synapses in the LPBel on skin cooling-evoked changes in sympathetic thermogenic activity by monitoring BAT SNA and BAT temperature, in metabolic rate by monitoring expired CO<sub>2</sub> and in cardiovascular tone by monitoring heart rate

and arterial pressure (Fig. 3). As reported<sup>5</sup>, cooling the trunk skin for 200–300 s consistently evoked rapid increases in BAT SNA, BAT temperature, expired CO<sub>2</sub> and heart rate with small changes in body core (rectal) and brain temperatures (Fig. 3a). During the rising phase of the skin cooling-evoked increase in these physiological parameters, muscimol, a widely used neuronal inhibitor<sup>21</sup>, or a mixture of AP5 and CNQX (AP5/CNQX), ionotropic glutamate receptor antagonists, was nano-injected bilaterally into the LPBel (Fig. 3b,g) and skin cooling was continued for at least 100 s after the nano-injections.

The muscimol or AP5/CNQX nano-injections into the LPBel completely reversed the skin cooling-evoked increases in BAT SNA, BAT temperature, expired CO<sub>2</sub> and heart rate to their resting levels by the end of the skin cooling episode (Fig. 3d,e,h). After the muscimol nano-injections, repeated skin cooling no longer evoked increases in these physiological parameters (Fig. 3a): the skin cooling-evoked increase in BAT SNA was  $1 \pm 0.3\%$  ( $n = 6$ ) of that before the injections. Bilateral AP5/CNQX nano-injections into the LPBel also completely blocked skin cooling-evoked shivering thermogenesis as monitored with electromyography (EMG) in skeletal muscle (Fig. 3f,i): the skin cooling-evoked EMG increase after the AP5/CNQX nano-injections into the LPB was  $0.2 \pm 1\%$  ( $n = 4$ ) of that before the injections. Bilateral muscimol nano-injections centered at a distance of 0.3–0.5 mm from the LPBel produced a partial inhibition (range: 10–70% inhibition) of the skin cooling-evoked increase in BAT SNA and muscimol nano-injections further away from the LPBel than these partially effective sites produced no inhibition (Fig. 3b), indicating that the LPBel is the most reactive LPB site for blockade of skin cooling-evoked increases in BAT SNA and that the effective diffusion sphere of muscimol was about 0.5 mm. When saline was nano-injected bilaterally into the LPBel, all the physiological variables increased throughout the skin cooling episode (Fig. 3c,h,i).

In contrast to the blockade of the skin cooling-evoked responses, none of the physiological responses evoked by a stimulation of thermogenic efferent pathways from the POA by prostaglandin E<sub>2</sub> (PGE<sub>2</sub>) were inhibited by bilateral muscimol nano-injections into the LPBel. The PGE<sub>2</sub>-evoked responses were, however, blocked by neuronal inhibition either of the DMH or the rostral medullary raphe (Supplementary Fig. 5), brain sites within thermogenic efferent pathways from the POA<sup>22–28</sup>. These results indicate that neuronal activation in the LPBel by cutaneous thermosensory signals, which is likely mediated by glutamatergic input from the dorsal horn, is required for the afferent, but not the efferent side of the skin cooling-triggered thermoregulatory reflex.

Supporting the concept that the LPB–POA pathway activated by cool signals from the skin mediates thermoregulatory responses, stimulation of LPBel neurons with a local nano-injection of NMDA consistently evoked short, but intense increases in BAT SNA, BAT temperature, expired CO<sub>2</sub>, heart rate and arterial pressure (Fig. 4). These responses were markedly reduced by pretreatment in the MnPO with AP5/CNQX: the inhibitory effect of AP5/CNQX was significantly different from that of saline (Fig. 4). This result also suggests that the LPB-mediated thermosensory pathway leading to thermogenic, metabolic and cardiovascular responses requires glutamatergic neurotransmission in the MnPO.

### Autonomic cold-defense does not require thalamic relay

The spinothalamocortical pathway is responsible for perception and discrimination of cutaneous temperature sensation<sup>9,10</sup>. To test the possibility that the spinothalamocortical pathway contributes to skin cooling-evoked homeostatic responses, we produced bilateral lesions in the ventral posteromedial and ventral posterolateral thalamic nuclei (VPM/VPL), which receive a majority of thermal somatosensory spinothalamic projections in rats<sup>29,30</sup>. The area lesioned with ibotenate injections, which covered most of the VPM/VPL, showed no immunoreactivity for NeuN, a neuronal marker, and was filled with small, glia-like cells as visualized with cresyl violet staining (Fig. 5a–c). The amplitude of the skin cooling-evoked

increase in BAT SNA in lesioned animals was not different from that in saline-injected control animals (Fig. 5d–f), indicating that the thermal afferent mechanism for skin cooling-evoked thermogenesis is independent of the spinothalamocortical pathway. To monitor the skin cooling-derived somatosensory input to the cerebral cortex, we simultaneously recorded electroencephalogram (EEG) from the primary somatosensory cortex. In the control animals, EEG activity was consistently increased by skin cooling and reversed to the basal level during rewarming, however, this skin temperature-dependent change in EEG activity was eliminated in the lesioned animals, confirming that the thalamic lesion ablated the spinothalamocortical pathway (Fig. 5d–f).

## DISCUSSION

How body temperature is defended against environmental thermal challenges is a fundamental question in physiology<sup>1,2</sup>. In the present study, we demonstrated, for the first time, the thermal somatosensory mechanism required for maintaining body temperature against environmental thermal challenges.

In this study, cold exposure of animals activated (induced Fos expression) many POA-projecting neurons distributed in the LPBel and LPBc. This observation suggests that such LPB neurons constitute a strong candidate population to provide thermosensory signals directly to the POA. Although this anatomical result itself does not exclude the possibility that the Fos expression was induced by factors secondary to thermal sensation, such as increased energy demand, this possibility seems unlikely based on our *in vivo* electrophysiological recording, in which most of the LPBel neurons projecting to the POA increased their firing rates promptly in response to skin cooling and the increases in their firing rates paralleled simultaneously evoked increases in BAT SNA.

Although the parabrachial area has been implicated in various homeostatic functions including thermogenesis<sup>15,31</sup>, little is known about how neurons in this area are functionally incorporated in the central neural circuits maintaining homeostasis. In our physiological study, inhibition of LPBel neurons or blockade of glutamate receptors in the LPBel completely suppressed sympathetic and shivering thermogenesis as well as metabolic and cardiac responses evoked by skin cooling. Furthermore, stimulation of LPBel neurons evoked physiological responses similar to those evoked by skin cooling and the responses by LPBel stimulation were dependent on glutamatergic neurotransmission in the POA. Based on these findings, we propose that cool signals originating from cutaneous thermoreceptors activate glutamate receptors on a population of neurons within the LPBel and LPBc, which, in turn, transmit these thermal signals to the POA, the thermoregulatory command center, through a direct glutamatergic projection (Supplementary Fig. 6).

Our anatomical observation of close appositions between the axon swellings of dorsal horn neurons and postsynaptic structures in LPB neurons projecting to the POA also supports the notion that POA-projecting LPB neurons are activated by direct glutamatergic inputs from second order somatosensory neurons in the dorsal horn (Supplementary Fig. 6). The glutamatergic innervation of LPB neurons by dorsal horn neurons is also consistent with anatomical findings that a substantial population of dorsal horn neurons provide their axon collaterals both to the LPB and thalamus<sup>32</sup> and their terminals in the thalamus contain glutamate<sup>33,34</sup>.

We have recently described the central efferent pathways from the POA that mediate skin cooling-evoked thermogenesis in BAT<sup>5</sup>. The thermogenic, metabolic and cardiac responses evoked by skin cooling are similar to those evoked by PGE<sub>2</sub>, a pyrogenic mediator, in the POA<sup>5,23,25,28</sup> and the brain regions that mediate the efferent drive from the POA leading to



skin cooling-evoked thermogenesis are also activated by PGE<sub>2</sub> in the POA<sup>5,22–28</sup>. Therefore, application of PGE<sub>2</sub> into the POA can stimulate the thermogenic efferent mechanism without altering the afferent signaling to the POA. In the present study, physiological responses evoked by PGE<sub>2</sub> in the POA were not affected by inhibition of LPB neurons, which, in contrast, completely blocked skin cooling-evoked homeostatic responses. These results indicate that activation of LPB neurons is essential for the afferent, but not the efferent arm of the thermoregulatory reflex triggered by skin cooling.

Although our CTb-Fos study did not reveal candidate neuronal populations providing direct thermosensory signals to the POA in any brain regions other than the LPB, it could have been possible that other neuronal populations, incompetent to express Fos, participated in thermosensory signaling to the POA. In addition, our results do not exclude the possibility that cool-responsive LPB neurons may have axonal branches that could bypass the POA, providing thermosensory signals directly to regions such as the DMH or the rostral medullary raphe that mediate thermoregulatory efferent signaling from the POA<sup>5,22–28</sup>. However, the potential roles of such pathways are minimized by the paucity of thermosensory projections from the LPB to the PVH and DMH as shown in our Fos-CTb study and by very few projections from the LPB to the rostral medullary raphe<sup>12</sup>. Furthermore, antagonizing glutamate receptors in the MnPO resulted in a nearly complete blockade of physiological responses to stimulation of LPB neurons in our study. These results emphasize the importance of the LPB–POA thermosensory signaling in the mechanism maintaining homeostasis against the impact of a reduced environmental temperature.

In classic studies, central thermosensation, mainly by POA neurons, was considered as a major thermosensory mechanism for body temperature control because the POA contains thermosensitive neurons<sup>1,2</sup>. As seen in our present and previous<sup>5</sup> studies, however, most thermoregulatory responses to changes in environmental temperature are rapidly evoked before brain temperature begins to change. In addition, brain temperature in conscious animals is not substantially changed during exposure to a cold (4°C) environment<sup>35</sup>. These observations highlight feedforward thermosensory signaling from the skin to the POA as a key mechanism in the defense of body temperature against environmental thermal challenges and our present data demonstrate that the spinal–LPB–POA pathway is an essential neural substrate for this feedforward signaling.

Of interest is how thermosensory afferent inputs from LPB neurons affect the activity of thermoregulatory neurons in the POA. Projection neurons in the POA controlling caudal thermogenic brain areas, such as the DMH and rostral medullary raphe, are thought to be inhibitory neurons that are tonically active when thermogenesis is not needed<sup>4,5,28</sup>. For example, transecting the output fibers from the POA activates BAT thermogenesis<sup>36</sup> and antagonizing GABA<sub>A</sub> receptors on neurons in the POA suppresses skin cooling-evoked BAT thermogenesis<sup>5</sup>. Thus, we reasoned that in order to increase thermogenesis, cutaneous cool signals ascending from the LPB and principally targeting the MnPO should drive a GABAergic inhibition of the tonically active, inhibitory POA projection neurons, the latter likely distributed both in the medial POA and the MnPO. Our finding that the LPB neurons activated by cutaneous cool signals provide an excitatory input, likely glutamatergic, to the MnPO is consistent with the existence of a population of inhibitory interneurons within the MnPO that, in turn, mediate a GABAergic inhibition of the tonic activity of the inhibitory projection neurons in the POA (Supplementary Fig. 6). Thus, the level of activity in the cooling-activated LPB–POA pathway regulates, through disinhibition, the activation of the pathways caudal to the POA that drive cold defense effectors (Supplementary Fig. 6). Consistent with the hypothetical existence of the MnPO interneurons, we have found that glutamatergic stimulation in the MnPO evokes thermogenic responses similar to those evoked by skin cooling, while stimulation in the medial or lateral POA does not (unpublished data).

The POA is also the site of pyrogenic action of PGE<sub>2</sub>. The EP3 subtype of PGE receptor, an inhibitory receptor, is somatodendritically distributed in the MnPO and medial POA<sup>37</sup> and ablation of most of these receptors largely attenuated fever<sup>38</sup>. Most of the EP3-expressing POA neurons are GABAergic and their caudal projection sites include the DMH and rostral medullary raphe<sup>22,28</sup>. Therefore, those inhibitory projection neurons in the POA that tonically inhibit the caudal thermogenic regions may express EP3 receptors and an action of PGE<sub>2</sub> on these receptors could attenuate their tonic activity, disinhibiting the caudal thermogenic regions and allowing fever to develop.

Spinothalamic and trigeminothalamic lamina I neurons, whose collaterals likely provide somatosensory signals to the LPB<sup>32,39</sup>, have been categorized into three classes: nociceptive-specific cells responding to noxious mechanical and heat stimuli; polymodal nociceptive cells responding to noxious mechanical, heat and cold stimuli; and thermoreceptive-specific cells responding linearly to graded, innocuous cooling or warming stimuli and not being activated further in the noxious temperature range<sup>40</sup>. In the present study of the thermoregulatory afferent pathway, we examined the responsiveness of LPB neurons specifically to innocuous skin cooling: in the physiological experiments, trunk skin temperature ranged from 27°C to 39°C and in the CTb-Fos study, the cold environment did not produce skin surface temperatures in the noxious cold range (< 15°C)<sup>35</sup>. The lack of responsiveness to noxious mechanical stimuli of the cool-responsive LPB neurons found in our unit recording suggests that they are primarily activated by thermoreceptive-specific dorsal horn neurons. Although LPB neurons that can be activated by cutaneous noxious stimuli have specific receptive fields on the body surface, the rat tail is included in the excitatory receptive fields of a dominant population of LPB nociceptor-responsive neurons in this species<sup>20</sup>. Thus, our conclusion from the tail pinch data, that most cool-responsive LPB neurons are not also involved in the transmission of noxious mechanical stimuli, is with the caveat that, due to the presence of the water jacket, we were unable to thoroughly examine nociceptive responses that might have been elicited from the trunk skin.

Cool-responsive LPB neurons in the present study showed an intriguing firing pattern in response to skin cooling and rewarming. Their firing rate showed a linear increase as the skin temperature was lowered between 36.6 and 34.4°C (a range just below the normal core temperature of rats), followed by a sustained elevation in discharge as the skin cooling was maintained. These consistent responses of cool-responsive LPB neurons to skin cooling mimic those observed in a skin cooling-responsive population of POA neurons<sup>41</sup>, providing further support for the primary role of LPB neurons in conveying cutaneous thermal information to thermoregulatory circuits in the POA. The elevated firing rate of the cool-responsive LPB neurons through the course of skin cooling was rapidly reduced to the basal level soon after skin rewarming was initiated, while skin temperatures were still low. This rapid inhibition by skin rewarming was also seen at the effector level (BAT SNA and EMG in the present study) and has been described at the level of thermoreceptive-specific lamina I cells mediating cool signals (COOL cells)<sup>40</sup>. This behavior may be accounted for by COOL cells that are activated by cool primary sensory fibers but also inhibited by warm primary sensory fibers. Under these conditions, a rapid increase in the activity of warm fibers upon skin rewarming<sup>42</sup> could rapidly suppress COOL cell discharge and, in turn, reduce the excitation of cool-responsive LPB neurons.

Within the framework of the somatosensory system, the spinothalamocortical pathway is well-known to mediate perception and discrimination of cutaneous temperature sensation<sup>9,10</sup> and the signals are relayed by thalamic neurons in the VPM/VPL in rats<sup>29,30</sup>. In the present study, lesions of the VPM/VPL had no effect on skin cooling-evoked thermogenesis, but eliminated skin temperature-dependent changes in EEG recorded from the primary somatosensory cortex. This result clearly indicates that the skin cooling-triggered feedforward thermosensory mechanism for controlling body temperature does not require a relay in the thalamus.

Therefore, we propose that the spinal-LPB-POA pathway be considered as a novel 'thermoregulatory afferent' pathway that is distinct from the spinothalamic pathway for conscious thermal sensations (Supplementary Fig. 6).

In addition to somatosensory signals, the LPB receives massive visceral afferent information through the nucleus of the solitary tract<sup>43</sup>. This suggests a potential role of the LPB-POA pathway in transmitting a broad array of visceral information (*e.g.*, gastric tension, satiety, taste, thirsty, blood pressure and temperature) to the POA, an important region for the control of many homeostatic conditions including energy expenditure, osmolarity and cardiovascular tone as well as body temperature<sup>5,44,45</sup>. Along this notion, LPB neurons might serve as a pivotal integrator of somatosensory and visceral information and such integration would be required for the orchestrated control of a variety of effectors that maintain homeostasis.

## METHODS

### Animals

Male Sprague-Dawley rats (200–500 g; Charles River) were housed with *ad libitum* access to food and water in a room air-conditioned at 22–23°C with a standard 12 h light/dark cycle. All procedures conform to the regulations detailed in the National Institutes of Health Guide for the Care and Use of Laboratory Animals and were approved by the Animal Care and Use Committee of the Oregon Health & Science University.

### CTb-Fos study

The detailed procedure of the CTb injection has been described<sup>28</sup>. Rats deeply anesthetized with chloral hydrate (280 mg/kg, *i.p.*) received a pressure-injection of 1.0 mg·ml<sup>-1</sup> Alexa594-conjugated CTb (70–120 nl; Molecular Probes) through a glass micropipette into the POA, BST, PVH or DMH. At the end of the surgery, 5 mg·ml<sup>-1</sup> penicillin G solution (200 µl) was injected into femoral muscles to avoid infection. The animals were caged individually and 3 or 4 d after the surgery, they were acclimatized to the chamber at 24°C for 3 d<sup>46</sup>. On the 4th day in the chamber, they were exposed to 4°C or 24°C for 4 h (from 10 A.M. to 2 P.M.). During the exposure to 4°C, the animals huddled, shivered and consumed food, but displayed no signs of discomfort, anxiety or pain. Immediately after the exposure, the animals were transcardially perfused with 4% formaldehyde and the brains were subjected to CTb and Fos immunohistochemistry.

### Dual tracer injection

Rats received a pressure-injection of 4% Fluoro-Gold (20–30 nl; Fluorochrome) into the POA using a Picospritzer II (General Valve) and an iontophoretic application of 2.5% PHA-L (pH 8.0 in 10 mM sodium phosphate buffer; Vector) into two sites in the mid-cervical spinal dorsal horn through a glass micropipette (tip inner diameter 10–15 µm) by applying a +2.0 µA constant current with 7-s on-off cycles for 10 min per site. Seven days after the surgery, the animals were perfused with 4% formaldehyde and the brains were subjected to fluorescence immunohistochemistry.

### Immunohistochemistry

Immunohistochemical procedures basically followed our previous studies<sup>22,28,46–48</sup>. After perfusion, the brain was postfixed, cryoprotected and cut into 30- or 40-µm-thick frontal sections. For single immunoperoxidase staining, an anti-NeuN mouse antibody (1 µg·ml<sup>-1</sup>; Chemicon) was used with a diaminobenzidine staining method<sup>47</sup>. For triple immunofluorescence staining, sections were incubated with a mixture of an anti-Fluorescent Gold rabbit antibody (1:5,000; Chemicon), an anti-PHA-L goat antibody (1 µg·ml<sup>-1</sup>; Vector)



and an anti-PSD-95 mouse antibody ( $1 \mu\text{g}\cdot\text{ml}^{-1}$ ; Chemicon) and then with a biotinylated donkey antibody to goat IgG (1:100). After blocking with 10% normal goat serum, the sections were incubated with  $10 \mu\text{g}\cdot\text{ml}^{-1}$  Alexa488-conjugated goat antibody to rabbit IgG,  $10 \mu\text{g}\cdot\text{ml}^{-1}$  Alexa647-conjugated goat antibody to mouse IgG and  $5 \mu\text{g}\cdot\text{ml}^{-1}$  Alexa546-conjugated streptavidin (Molecular Probes). The sections were observed under a confocal laser-scanning microscope (LSM510; Zeiss). Double immunoperoxidase staining for CTb and Fos and PHA-L and Fluoro-Gold followed our previous method<sup>22,46</sup>.

## Anatomy

The nomenclature of LPB subnuclei basically followed that in a previous study<sup>13</sup>, except for inclusion of the ventral subnucleus into the LPBc.

## Lesion

Rats received bilateral injections of 50 mM ibotenate or saline (60–120 nl per site) into 6 sites per side throughout the VPM/VPL (3.0–3.8 mm caudal to bregma). The animals survived for at least 1 week and were then subjected to *in vivo* physiological experiments.

## *In vivo* physiology

The procedures for the animal preparation and skin cooling experiments have been previously described<sup>5</sup>. Rats were anesthetized with intravenous urethane ( $0.8 \text{ g}\cdot\text{kg}^{-1}$ ) and  $\alpha$ -chloralose ( $70 \text{ mg}\cdot\text{kg}^{-1}$ ), paralyzed with D-tubocurarine, and artificially ventilated with 100% O<sub>2</sub>. The trunk was shaved, a thermocouple to monitor skin temperature was taped onto the abdominal skin, and the trunk was wrapped with a plastic water jacket to cool and rewarm the skin. Postganglionic BAT SNA was recorded from the right interscapular BAT pad. Nerve activity was filtered (1–300 Hz) and amplified ( $\times 5,000$ – $50,000$ ) with a CyberAmp 380 (Axon Instruments). Physiological variables were digitized and recorded to a computer hard disk using Spike 2 software (CED).

For recording EMG or EEG, rats were anesthetized with 2.0% isoflurane in 100% O<sub>2</sub> through a tracheal cannula with the animal's spontaneous ventilation. Bipolar needle electrodes for EMG were inserted into muscles of dorsal neck. Bipolar electrodes for EEG recording were placed in the primary somatosensory cortex (0.5 or 2.5 mm posterior to bregma, 3.0 mm lateral (right) to the midline and 1.0 mm ventral to the brain surface). During EMG or EEG measurement, the isoflurane concentration was decreased to 0.6% and under this anesthetic condition without paralysis, the animals never showed any movement except for cooling-evoked shivering. EMG and EEG signals were amplified and filtered (EMG:  $\times 5,000$ , 10–1,000 Hz; EEG:  $\times 10,000$ , 1–30 Hz).

Spike 2 software was used to obtain a continuous measure (4-s bins) of BAT SNA, EMG and EEG amplitude by calculating the root mean square amplitude of these variables (square root of the total power in the 0–20 Hz band for BAT SNA, 0–500 Hz band for EMG and 0.5–2.5 Hz band for EEG) from the autospectra of sequential 4-s segments of these variables.

Stereotaxic pressure-injection of drugs into the brain in nanoliter volumes (nanoinjections) was performed using glass micropipettes (tip inner diameter, 20–30  $\mu\text{m}$ ) as described<sup>5</sup>. The concentrations of injected drugs were muscimol (2 mM), AP5/CNQX (5 mM each) and NMDA (0.2 mM) and the doses followed our previous *in vivo* physiological studies<sup>5,22,23,25,28,46</sup>, in which we obtained consistent effects from these drug doses. To mark the injection sites, fluorescent microspheres (Molecular Probes) were injected at the same stereotaxic coordinates through the same micropipette as described<sup>5</sup>. After the physiological recordings, the animals were perfused with 10% formaldehyde and the brain tissues were sectioned. The locations of

the nanoinjections were identified by detecting the fluorescent microspheres in the sections under an epifluorescence microscope.

In the analysis of data from skin cooling experiments (Fig. 3h,i), baseline values of the physiological variables were the averages during the 1-min period immediately prior to skin cooling (before cooling). Skin cooling-evoked response values for BAT temperature, expired CO<sub>2</sub> and heart rate were taken just prior to the first of the bilateral intra-LPB nanoinjections, and those for BAT SNA, mean arterial pressure and EMG were the averages during the 1-min period immediately prior to the first nanoinjection (1st injection). Drug treatment effect values for BAT temperature, expired CO<sub>2</sub> and heart rate were taken at the end of skin cooling, and those for BAT SNA, mean arterial pressure and EMG were the averages during the 1-min period immediately prior to the end of skin cooling (end of cooling).

In the analysis of data from experiments involving nanoinjection of NMDA into the LPB (Fig. 4b), each animal had a unilateral NMDA injection in the LPB following saline-pretreatment in the MnPO and then another NMDA injection in the LPB following AP5/CNQX-pretreatment in the MnPO and all the repeated injections were made at the same sites. For BAT temperature, expired CO<sub>2</sub>, heart rate and mean arterial pressure, NMDA-evoked changes from their baseline to peak values within 4 min after the NMDA injection were calculated. For BAT SNA, the area under the curve (AUC) of the 'power per 4 s' trace above the baseline for 4 min after the NMDA injection (subtracted AUC) was calculated. Baseline values of all these physiological variables were taken as the averages during the 1-min period immediately prior to the NMDA injection.

### Unit recording

Rats received urethane and  $\alpha$ -chloralose anesthesia. Unit recordings were made with glass microelectrodes filled with 0.5 M sodium acetate (DC resistance: 20–44 M $\Omega$ ) containing 5% biotinamide to allow juxtacellular labeling of the recorded neurons. A monopolar tungsten stimulating microelectrode was stereotaxically positioned in the MnPO. The LPB was explored for neurons showing a constant onset latency response to electrical stimulation in the POA (0.3–4 mA, 1 ms, 0.25–0.33 Hz). Standard criteria<sup>49</sup> were used to establish the antidromic nature of the responses of LPB neurons to POA stimulation. After time-controlled collision tests (Fig. 2b), the thermosensitivity of LPB neurons was tested by cooling the skin for 100–300 s and this cooling challenge was repeated at least twice. For juxtacellular labeling<sup>50</sup> of the recorded neurons with biotinamide, positive current pulses (0.5–4.0 nA, 400 ms duration, 50% duty cycle) were delivered for 1–5 min to entrain the neuron. After the recording, the animals were perfused with 4% formaldehyde and the labeled neurons were visualized by incubating the brain sections with 1  $\mu\text{g}\cdot\text{ml}^{-1}$  Alexa594-conjugated streptavidin. For firing rate analysis of each recorded neuron, the rate of spontaneous firing was measured as spikes $\cdot 10\text{ s}^{-1}$  and all response values represent the average of the 2 skin cooling episodes.

### Statistics

Statistical significance was evaluated with a two-tailed paired or unpaired *t*-test or a one-way analysis of variance (ANOVA) for between-group significance with a Bonferroni *post hoc* test to detect pairwise differences. Analysis of correlation between unit firing rate and skin temperature was performed using Pearson's correlation test.

### Supplementary Material

Refer to Web version on PubMed Central for supplementary material.

### Acknowledgements

This work was supported by US National Institutes of Health (NIH) grants NS40987 and DK57838 to S.F.M. K.N. is a fellow for research abroad supported by the Japan Society for the Promotion of Science. Acquisition of confocal images was supported by NIH instrumentation grant RR016858. We thank Dr. Yoshiko Nakamura for her inspiring discussion and assistance.

### References

1. Hammel HT. Regulation of internal body temperature. *Annu Rev Physiol* 1968;30:641–710. [PubMed: 4871163]
2. Hensel, H. Thermoreception and temperature regulation. Monographs of the Physiological Society No. 38. Academic press; London: 1981.
3. Boulant JA, Gonzalez RR. The effect of skin temperature on the hypothalamic control of heat loss and heat production. *Brain Res* 1977;120:367–372. [PubMed: 832130]
4. Nagashima K, Nakai S, Tanaka M, Kanosue K. Neuronal circuitries involved in thermoregulation. *Auton Neurosci* 2000;85:18–25. [PubMed: 11189023]
5. Nakamura K, Morrison SF. Central efferent pathways mediating skin cooling-evoked sympathetic thermogenesis in brown adipose tissue. *Am J Physiol* 2007;292:R127–R136.
6. Romanovsky AA. Thermoregulation: some concepts have changed. Functional architecture of the thermoregulatory system. *Am J Physiol* 2007;292:R37–R46.
7. Huckaba CE, Downey JA, Darling RC. A feedback-feedforward mechanism describing the interaction of central and peripheral signals in human thermoregulation. *Int J Biometeorol* 1971;15:141–145. [PubMed: 5146799]
8. Savage MV, Brengelmann GL. Control of skin blood flow in the neutral zone of human body temperature regulation. *J Appl Physiol* 1996;80:1249–1257. [PubMed: 8926253]
9. Craig AD, Bushnell MC, Zhang ET, Blomqvist A. A thalamic nucleus specific for pain and temperature sensation. *Nature* 1994;372:770–773. [PubMed: 7695716]
10. Craig AD. How do you feel? Interoception: the sense of the physiological condition of the body. *Nat Rev Neurosci* 2002;3:655–666. [PubMed: 12154366]
11. Sagar SM, Sharp FR, Curran T. Expression of *c-fos* protein in brain: metabolic mapping at the cellular level. *Science* 1988;240:1328–1331. [PubMed: 3131879]
12. Saper CB, Loewy AD. Efferent connections of the parabrachial nucleus in the rat. *Brain Res* 1980;197:291–317. [PubMed: 7407557]
13. Fulwiler CE, Saper CB. Subnuclear organization of the efferent connections of the parabrachial nucleus in the rat. *Brain Res Rev* 1984;7:229–259.
14. Krukoff TL, Harris KH, Jhamandas JH. Efferent projections from the parabrachial nucleus demonstrated with the anterograde tracer *Phaseolus vulgaris* leucoagglutinin. *Brain Res Bull* 1993;30:163–172. [PubMed: 7678381]
15. Bester H, Besson JM, Bernard JF. Organization of efferent projections from the parabrachial area to the hypothalamus: a *Phaseolus vulgaris*-leucoagglutinin study in the rat. *J Comp Neurol* 1997;383:245–281. [PubMed: 9205041]
16. Lumpkin EA, Caterina MJ. Mechanisms of sensory transduction in the skin. *Nature* 2007;445:858–865. [PubMed: 17314972]
17. Cechetto DF, Standaert DG, Saper CB. Spinal and trigeminal dorsal horn projections to the parabrachial nucleus in the rat. *J Comp Neurol* 1985;240:153–160. [PubMed: 3840498]
18. Bernard JF, Dallel R, Raboisson P, Villanueva L, Le Bars D. Organization of the efferent projections from the spinal cervical enlargement to the parabrachial area and periaqueductal gray: a PHA-L study in the rat. *J Comp Neurol* 1995;353:480–505. [PubMed: 7759612]
19. Feil K, Herbert H. Topographic organization of spinal and trigeminal somatosensory pathways to the rat parabrachial and Kölliker-Fuse nuclei. *J Comp Neurol* 1995;353:506–528. [PubMed: 7759613]
20. Bester H, Menendez L, Besson JM, Bernard JF. Spino(trigemino)parabrachiohypothalamic pathway: electrophysiological evidence for an involvement in pain processes. *J Neurophysiol* 1995;73:568–585. [PubMed: 7760119]

21. Johnston GAR. GABA<sub>A</sub> receptor pharmacology. *Pharmacol Ther* 1996;69:173–198. [PubMed: 8783370]
22. Nakamura K, et al. The rostral raphe pallidus nucleus mediates pyrogenic transmission from the preoptic area. *J Neurosci* 2002;22:4600–4610. [PubMed: 12040067]
23. Madden CJ, Morrison SF. Excitatory amino acid receptor activation in the raphe pallidus area mediates prostaglandin-evoked thermogenesis. *Neuroscience* 2003;122:5–15. [PubMed: 14596844]
24. Zaretskaia MV, Zaretsky DV, DiMicco JA. Role of the dorsomedial hypothalamus in thermogenesis and tachycardia caused by microinjection of prostaglandin E<sub>2</sub> into the preoptic area in anesthetized rats. *Neurosci Lett* 2003;340:1–4. [PubMed: 12648744]
25. Madden CJ, Morrison SF. Excitatory amino acid receptors in the dorsomedial hypothalamus mediate prostaglandin-evoked thermogenesis in brown adipose tissue. *Am J Physiol* 2004;286:R320–R325.
26. Nakamura K. Fever-inducing sympathetic neural pathways. *J Therm Biol* 2004;29:339–344.
27. Nakamura K, Matsumura K, Kobayashi S, Kaneko T. Sympathetic premotor neurons mediating thermoregulatory functions. *Neurosci Res* 2005;51:1–8. [PubMed: 15596234]
28. Nakamura Y, et al. Direct pyrogenic input from prostaglandin EP3 receptor-expressing preoptic neurons to the dorsomedial hypothalamus. *Eur J Neurosci* 2005;22:3137–3146. [PubMed: 16367780]
29. Gauriau C, Bernard JF. A comparative reappraisal of projections from the superficial laminae of the dorsal horn in the rat: the forebrain. *J Comp Neurol* 2004;468:24–56. [PubMed: 14648689]
30. Zhang X, Davidson S, Giesler GJ Jr. Thermally identified subgroups of marginal zone neurons project to distinct regions of the ventral posterior lateral nucleus in rats. *J Neurosci* 2006;26:5215–5223. [PubMed: 16687513]
31. Kobayashi A, Osaka T. Involvement of the parabrachial nucleus in thermogenesis induced by environmental cooling in the rat. *Pflügers Arch* 2003;446:760–765.
32. Hylden JLK, Anton F, Nahin RL. Spinal lamina I projection neurons in the rat: collateral innervation of parabrachial area and thalamus. *Neuroscience* 1989;28:27–37. [PubMed: 2548118]
33. Broman J, Ottersen OP. Cervicothalamic tract terminals are enriched in glutamate-like immunoreactivity: an electron microscopic double-labeling study in the cat. *J Neurosci* 1992;12:204–221. [PubMed: 1370321]
34. Blomqvist A, Ericson AC, Craig AD, Broman J. Evidence for glutamate as a neurotransmitter in spinothalamic tract terminals in the posterior region of owl monkeys. *Exp Brain Res* 1996;108:33–44. [PubMed: 8721153]
35. Bratincsák A, Palkovits M. Evidence that peripheral rather than intracranial thermal signals induce thermoregulation. *Neuroscience* 2005;135:525–532. [PubMed: 16125855]
36. Chen XM, Hosono T, Yoda T, Fukuda Y, Kanosue K. Efferent projection from the preoptic area for the control of non-shivering thermogenesis in rats. *J Physiol (Lond)* 1998;512:883–892. [PubMed: 9769429]
37. Nakamura K, et al. Immunocytochemical localization of prostaglandin EP3 receptor in the rat hypothalamus. *Neurosci Lett* 1999;260:117–120. [PubMed: 10025713]
38. Lazarus M, et al. EP3 prostaglandin receptors in the median preoptic nucleus are critical for fever responses. *Nat Neurosci* 2007;10:1131–1133. [PubMed: 17676060]
39. Bester H, Chapman V, Besson JM, Bernard JF. Physiological properties of the lamina I spinoparabrachial neurons in the rat. *J Neurophysiol* 2000;83:2239–2259. [PubMed: 10758132]
40. Craig AD, Dostrovsky JO. Differential projections of thermoreceptive and nociceptive lamina I trigeminothalamic and spinothalamic neurons in the cat. *J Neurophysiol* 2001;86:856–870. [PubMed: 11495956]
41. Boulant JA, Hardy JD. The effect of spinal and skin temperatures on the firing rate and thermosensitivity of preoptic neurones. *J Physiol (Lond)* 240:639–660. [PubMed: 4416218]
42. Hellon RF, Hensel H, Schäfer K. Thermal receptors in the scrotum of the rat. *J Physiol (Lond)* 1975;248:349–357. [PubMed: 1151787]
43. Saper CB. The central autonomic nervous system: conscious visceral perception and autonomic pattern generation. *Annu Rev Neurosci* 2002;25:433–469. [PubMed: 12052916]

44. Hori T, Nakashima T, Koga H, Kiyohara T, Inoue T. Convergence of thermal, osmotic and cardiovascular signals on preoptic and anterior hypothalamic neurons in the rat. *Brain Res Bull* 1988;20:879–885. [PubMed: 3044527]
45. Morrison SF. Central pathways controlling brown adipose tissue thermogenesis. *News Physiol Sci* 2004;19:67–74. [PubMed: 15016906]
46. Nakamura K, et al. Identification of sympathetic premotor neurons in medullary raphe regions mediating fever and other thermoregulatory functions. *J Neurosci* 2004;24:5370–5380. [PubMed: 15190110]
47. Nakamura K, et al. Immunohistochemical localization of prostaglandin EP3 receptor in the rat nervous system. *J Comp Neurol* 2000;421:543–569. [PubMed: 10842213]
48. Nakamura K, Li YQ, Kaneko T, Katoh H, Negishi M. Prostaglandin EP3 receptor protein in serotonin and catecholamine cell groups: a double immunofluorescence study in the rat brain. *Neuroscience* 2001;103:763–775. [PubMed: 11274793]
49. Morrison SF, Cao WH. Different adrenal sympathetic preganglionic neurons regulate epinephrine and norepinephrine secretion. *Am J Physiol* 2000;279:R1763–R1775.
50. Pinault D. A novel single-cell staining procedure performed in vivo under electrophysiological control: morpho-functional features of juxtacellularly labeled thalamic cells and other central neurons with biocytin or Neurobiotin. *J Neurosci Methods* 1996;65:113–136. [PubMed: 8740589]



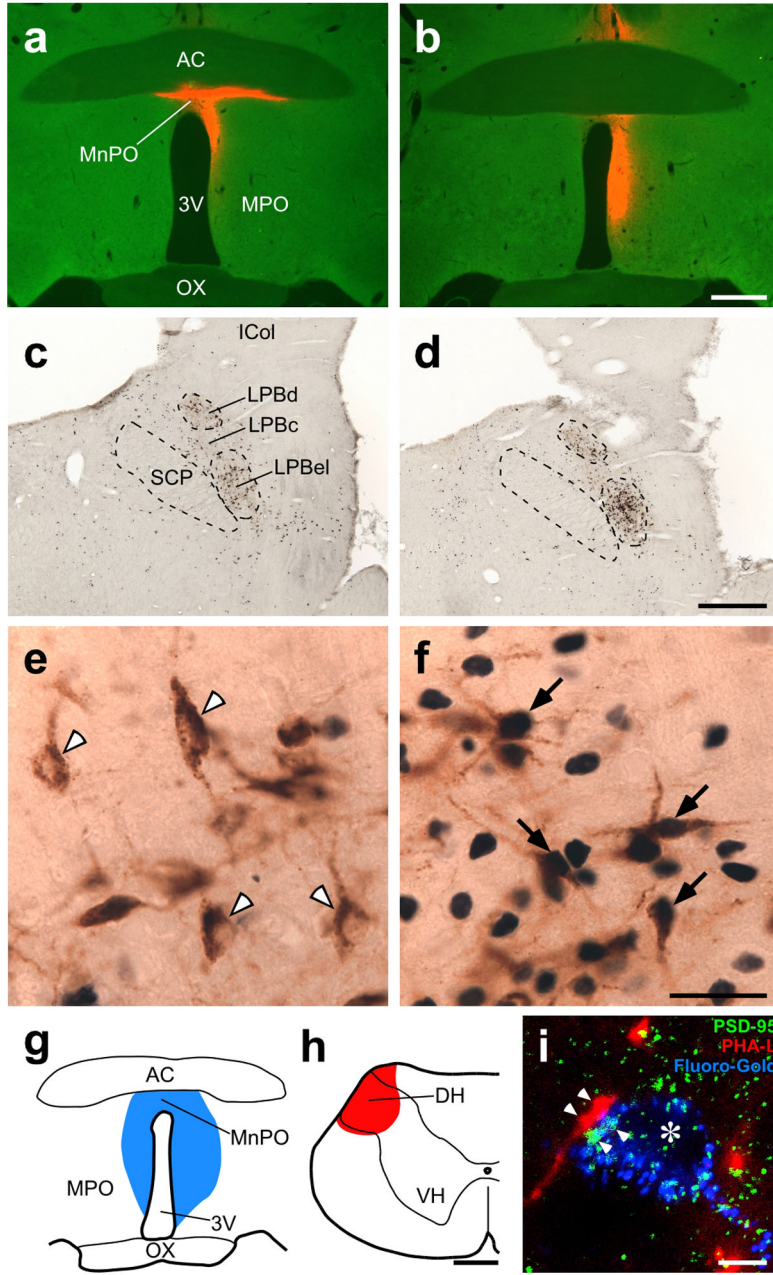


**Figure 1.** POA-projecting LPB neurons are activated in a cold environment and innervated by dorsal horn (DH) neurons. (a–f) Fos expression in LPB neurons retrogradely labeled with CTb injected into the POA in animals exposed to 24°C (a,c,e) and 4°C (b,d,f). a and b show injection sites of CTb (red). In c–f, CTb (brown) and Fos (blue-black) immunoreactivities in the LPB of the animals shown in a and b were visualized. In e and f, arrowheads indicate Fos-negative, CTb-labeled neurons and arrows indicate Fos-positive, CTb-labeled neurons. 3V, third ventricle; AC, anterior commissure; ICol, inferior colliculus; MPO, medial preoptic area; OX, optic chiasm; SCP, superior cerebellar peduncle. Scale bars, 0.5 mm (a–d), 30 μm (e,f). (g–i) Dual tracing experiment using Fluoro-Gold (blue) injected into the POA (g) and PHA-L (red) injected into the spinal cervical DH (h). Confocal image from the LPBel (i) shows axon

swellings, anterogradely labeled with PHA-L from the DH, closely associated (arrowheads) with PSD-95-positive (green) postsynaptic structures within LPB neurons retrogradely labeled with Fluoro-Gold from the POA. The signals for these three labelings are displayed using pseudo-colors. Asterisk indicates the cell nucleus of a Fluoro-Gold-labeled LPB neuron. VH, ventral horn. Scale bars, 0.5 mm (**g,h**), 5  $\mu$ m (**i**).

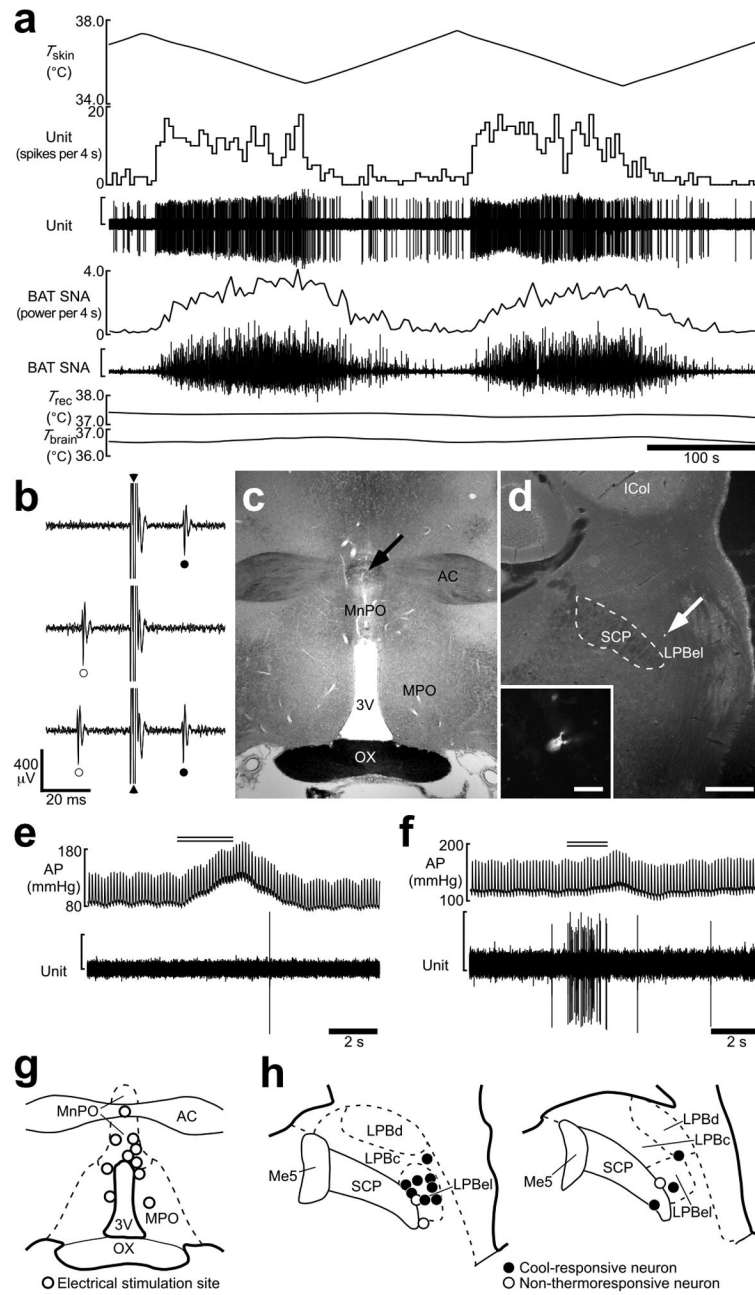


**Figure 2.**

Skin cooling-evoked response of single LPB neurons antidromically activated from the POA. (a) *In vivo* extracellular unit recording of the action potentials of an LPB neuron (unit) and changes in BAT SNA, rectal temperature ( $T_{rec}$ ) and brain temperature ( $T_{brain}$ ) in response to trunk skin cooling ( $T_{skin}$ ). The vertical scale bars for the unit and BAT SNA traces represent 300  $\mu$ V and 100  $\mu$ V, respectively. Note that  $T_{rec}$  and  $T_{brain}$  do not change substantially during skin cooling and rewarming. (b) Collision test for the LPB neuron shown in a. Single pulse stimulation in the POA (triangle) evoked a constant-onset latency (20 ms) response in this neuron (filled circle, top trace). POA stimulation at 19 ms after a spontaneous action potential (open circle) failed to evoke a response of this neuron (middle trace). POA stimulation at 21 ms after a spontaneous action potential evoked a constant-onset latency response of this neuron

(bottom trace). All traces are superpositions of 3 stimulation trials. **(c)** The site of electrical stimulation for the collision tests in **b**. The site is identified by a small scar at the site of electrical stimulation (arrow). **(d)** Juxtacellular labeling allows visualization of the LPB neuron (arrow) from **a**. Inset, a magnified picture of this neuron. Scale bars, 0.5 mm (**c,d**), 30  $\mu\text{m}$  (inset in **d**). **(e,f)** Effect of tail pinch on firing activities of a cool-responsive neuron (**e**; the same neuron shown in **a**) and a non-thermoreponsive neuron (**f**). Double horizontal lines indicate the period of tail pinch. Note that tail pinch evoked a pressor response in both cases. The vertical scale bars for the unit traces in **e** and **f** represent 200  $\mu\text{V}$ . **(g)** Sites of electrical stimulation in the POA. **(h)** Locations of LPB neurons that were juxtacellularly labeled after unit recording. Neurons antidromically activated with electrical stimulation in the POA are categorized in terms of their responsiveness to skin cooling. Me5, mesencephalic trigeminal nucleus.

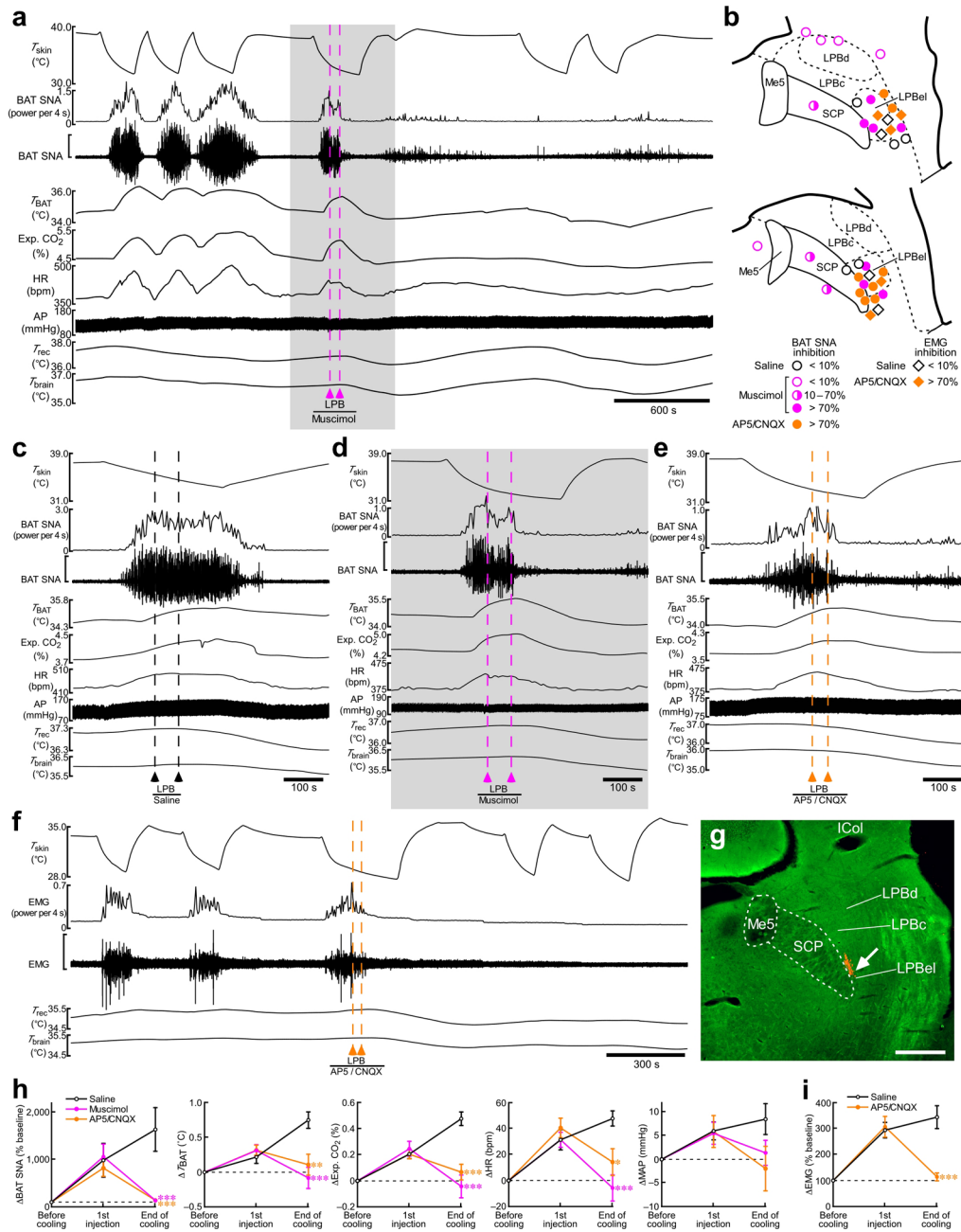


**Figure 3.** Inhibition of neuronal activity or blockade of ionotropic glutamate receptors in the LPB reverses skin cooling-evoked thermogenic, metabolic and cardiac responses. **(a)** Skin cooling-evoked changes in BAT SNA, BAT temperature ( $T_{BAT}$ ), expired (Exp.)  $CO_2$ , heart rate (HR), arterial pressure (AP),  $T_{rec}$ , and  $T_{brain}$  before and after bilateral nano-injections of muscimol into the LPB (pink dashed lines). The gray area is expanded in **d**. The vertical scale bar for the BAT SNA trace represents  $100 \mu V$ . **(b)** Composite drawing of sites of saline, muscimol (2 mM) or AP5/CNQX (5 mM each) nano-injections (60 nl) in and around the LPB with their inhibitory effects on the skin cooling-evoked increase in BAT SNA or EMG. The right side of the symmetric bilateral injections is shown. **(c-e)** Effect of bilateral nano-injections of saline **(c)**, muscimol **(d)** and AP5/CNQX **(e)** into the LPB on skin cooling-evoked changes in



physiological variables. The vertical scale bar for the BAT SNA trace represents 200  $\mu\text{V}$  (**c**), 100  $\mu\text{V}$  (**d**) and 50  $\mu\text{V}$  (**e**). (**f**) Skin cooling-evoked changes in EMG before and after bilateral nano-injections of AP5/CNQX into the LPB (orange dashed lines). The vertical scale bar for the EMG trace represents 400  $\mu\text{V}$ . **g**, Representative view of a nano-injection site in the LPBel as identified with a cluster of fluorescent beads (arrow). Scale bar, 0.5 mm. (**h,i**) Group data (mean  $\pm$  s.e.m.) showing the effect of saline ( $n = 5$ ), muscimol ( $n = 7$ ) or AP5/CNQX ( $n = 8$ ) nano-injections into the LPBel on skin cooling-evoked changes in BAT SNA,  $T_{\text{BAT}}$ , Exp.  $\text{CO}_2$ , HR and MAP (**h**) and the effect of saline ( $n = 4$ ) and AP5/CNQX ( $n = 5$ ) nano-injections into the LPBel on skin cooling-evoked changes in EMG (**i**) (see **c-f**). \* $P < 0.05$ ; \*\* $P < 0.01$ ; \*\*\* $P < 0.001$ , compared with the saline-injected group (Bonferroni *post hoc* test following a one-way factorial ANOVA).

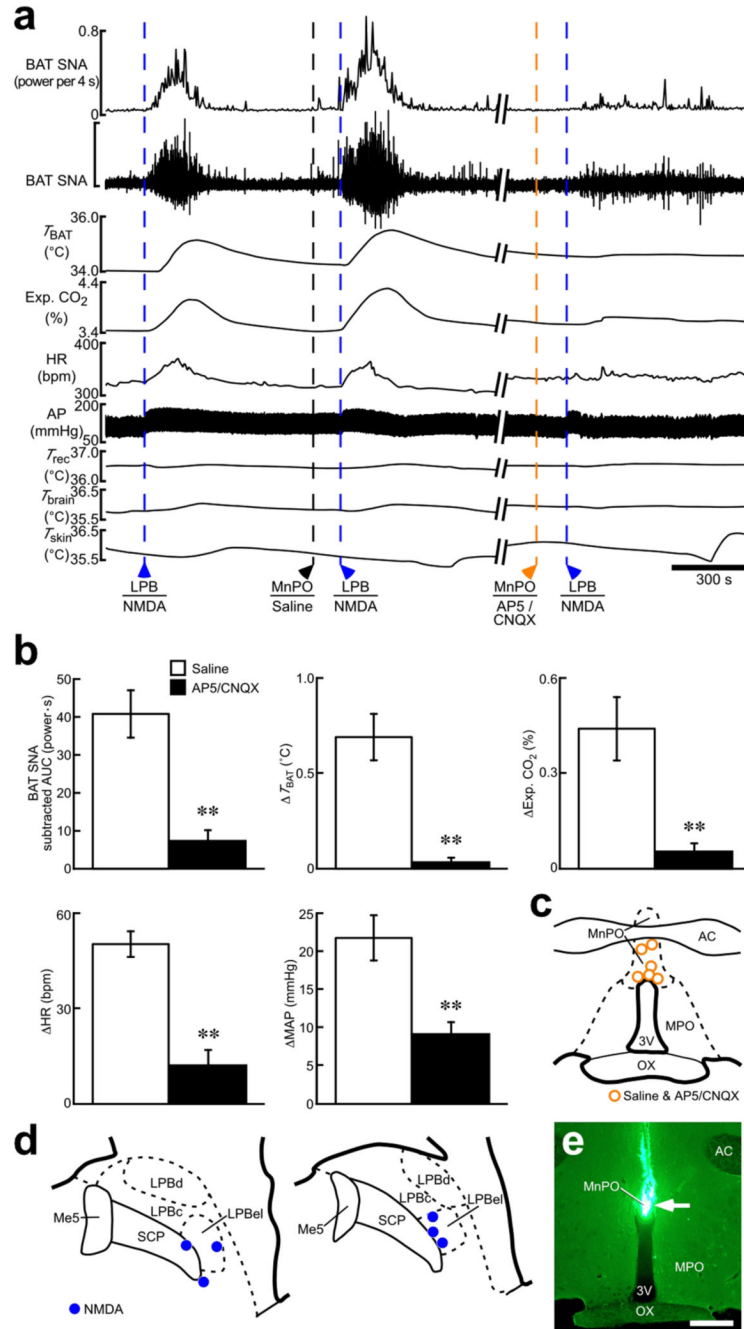


**Figure 4.** Stimulation of LPB neurons evokes thermogenic, metabolic and cardiovascular responses dependent on glutamatergic neurotransmission in the POA. **(a)** Effect of AP5/CNQX application (5 mM each, 100–200 nl) into the MnPO on thermogenic, metabolic and cardiovascular responses evoked by NMDA nanoinjection (0.2 mM, 36 nl) into the LPBel. The vertical scale bar for the BAT SNA trace represents 900  $\mu V$ . **(b)** Group data (mean  $\pm$  s.e.m.) showing the effect of pretreatment in the MnPO with saline or AP5/CNQX on increases in BAT SNA,  $T_{BAT}$ , Exp.  $CO_2$ , HR and MAP evoked by NMDA nanoinjection into the LPB. Each animal had an NMDA injection in the LPB following saline-pretreatment in the MnPO and then another NMDA injection in the LPB following AP5/CNQX-pretreatment in the MnPO

and all the repeated injections were made at the same sites.  $**P < 0.01$ ,  $n = 6$  (two-tailed paired  $t$ -test). **(c,d)** Sites of injections of saline and AP5/CNQX into the MnPO **(c)** and of NMDA into the LPB **(d)**. **(e)** Representative view of a nanoinjection site into the MnPO as identified with a cluster of fluorescent beads (arrow). Scale bar, 0.5 mm.

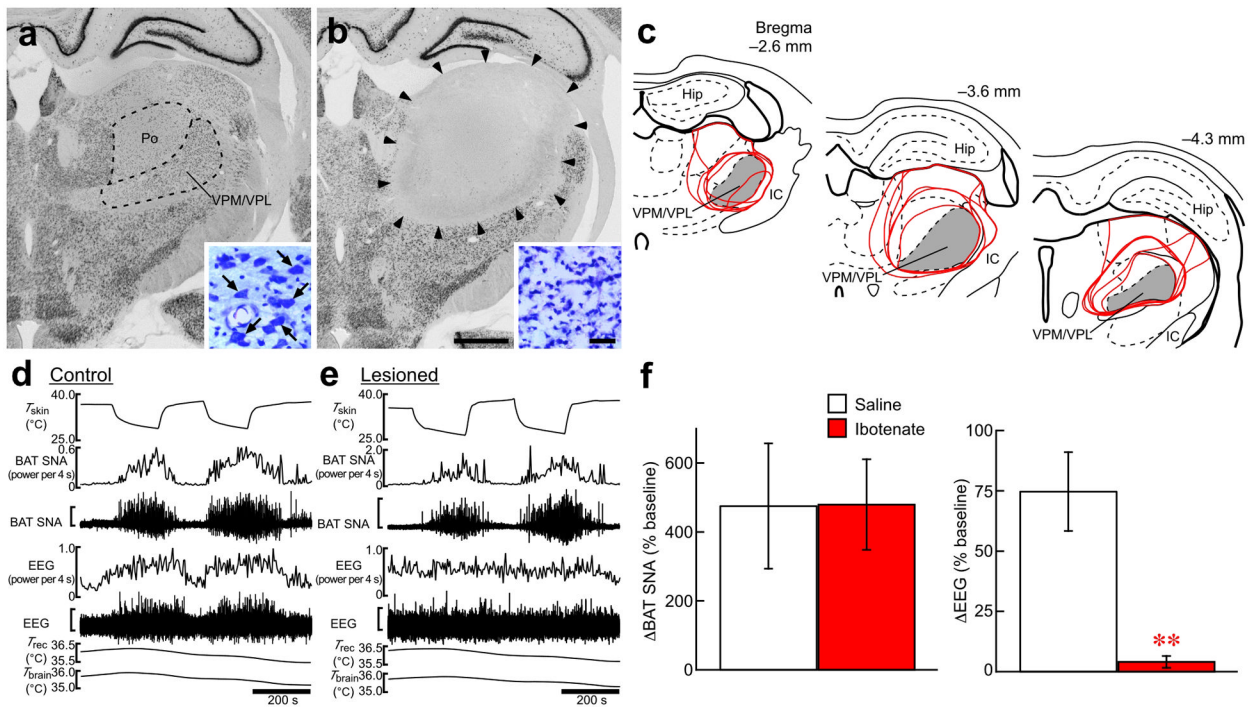


**Figure 5.**

Skin cooling-evoked thermogenic response does not require a thalamic relay. **(a,b)** NeuN immunohistochemistry and cresyl violet staining (insets) in the thalamus of a control **(a)** and of a thalamic-lesioned **(b)** animal. Ibotenate injections eliminated neurons in an area including the VPM/VPL and posterior thalamic nuclear group (Po) **(b)**, delineated by arrowheads as compared with the saline-injected control **(a)**. One side of the bilateral ibotenate or saline injection sites is shown. Large, neuron-like cells are found in the VPM/VPL of control animals **(a, inset, arrows)**, but not of lesioned animals, which contained gliosis **(b, inset)**. Scale bars, 1 mm **(a,b)**, 30  $\mu$ m (insets). **(c)** Thalamic area lesioned with ibotenate injections. Lesioned areas from all the animals are delineated with red lines and overlaid at three rostrocaudal levels. Gray area indicates the VPM/VPL. The right side of the bilateral symmetric lesions is shown. Hip, hippocampus; IC, internal capsule. **(d,e)** Skin cooling-evoked changes in BAT SNA and EEG in the animals from **a** and **b**. The vertical scale bars for the BAT SNA and EEG traces represent 25  $\mu$ V and 200  $\mu$ V **(d)** and 100  $\mu$ V and 200  $\mu$ V **(e)**, respectively. **(f)** Group data (mean  $\pm$  s.e.m.) showing the effect of the thalamic lesion on skin cooling-evoked changes in BAT SNA (saline,  $n = 5$ ; ibotenate,  $n = 6$ ) and EEG (saline,  $n = 3$ ; ibotenate,  $n = 5$ ). Skin cooling-evoked changes from the pre-cooling baseline to average value during the 1-min period immediately prior to the end of skin cooling (averaged from 2 cooling episodes in each animal) are shown. **\*\*** $P < 0.01$  (two-tailed unpaired  $t$ -test).